



16 October 2002

**CHEMICAL
PHYSICS
LETTERS**

Chemical Physics Letters 364 (2002) 556–561

www.elsevier.com/locate/cplett

Collective excitation dynamics and polaron formation in molecular aggregates

M. Dahlbom, W. Beenken, V. Sundström, T. Pullerits *

Department of Chemical Physics, Lund University, Box 124 S-211 00 Lund, Sweden

Received 25 April 2002; in final form 21 August 2002

Abstract

Real-space collective excitation dynamics in molecular aggregates is studied using a model where the electronic system is described via exciton theory with surface hopping. The nuclear dynamics are included using the Langevin equation where temperature and zero-point motions are entered via the fluctuation-dissipation theorem. Dynamic processes like exciton relaxation, localization, polaron formation and diffusion of self-trapped excitons, which commonly require different theories, are simultaneously described with our approach. Numerical simulations of small linear aggregates are performed. Contrary to the common view we show that exciton relaxation can temporarily increase exciton delocalization. The results are discussed based on the photosynthetic light-harvesting pigment-protein complexes.

© 2002 Elsevier Science B.V. All rights reserved.

1. Introduction

The concept of molecular excitons was introduced early in the last century and has been applied successfully to a large number of different systems, for example the photosynthetic light-harvesting antenna complexes [1]. An exciton is a collective electronic excitation extended over many molecules due to the excited state transfer interaction. The degree of delocalization is balanced by the static energy disorder and the exciton–phonon coupling. The latter leads to new quasi-particles,

excitonic polarons. For simplicity, we will use polarons here. The polaron states are excitons dressed with a phonon cloud. Polarons can be trapped at lattice sites (self-trapping) due to the displacement of the excited state potential caused by deformation of the surrounding environment induced by the exciton–phonon coupling [2]. There exists extensive literature about polarons in various materials with different coupling regimes, dating back several tens of years [3–7].

A number of different techniques have been utilized in order to characterize the properties of the excitons in the B850 antenna aggregate of the peripheral light-harvesting complex (LH2) from purple bacteria [8]. It has been proposed that the initially created exciton may span a considerable size of the aggregate and relax within a few

* Corresponding author. Fax: +46-46-2224119.

E-mail address: tonu.pullerits@chemphys.lu.se (T. Pullerits).

hundreds of femtoseconds to an equilibrium size of just a few molecular sites [9]. A red spectral feature recorded with transient absorption spectroscopy of the B850 aggregate at cryogenic temperatures has been proposed to originate from polaron formation [10]. Recently, a similar conclusion was drawn based on low temperature selectively excited fluorescence of B850 [11].

Previous methods to describe excitation dynamics in light-harvesting systems include the Redfield approach and the Holstein model. In the weak electron–phonon coupling limit the Redfield approach [12–14] is applicable. It captures the exciton relaxation between stationary exciton states. The Holstein model covers the strong-coupling case and describes phenomena such as polaron formation and self-trapping. It has been applied either using the cumulant expansion [15] or the long-time limit where the system is thermalized [16]. In this Letter, we present a novel description of exciton relaxation and polaron dynamics based on the electronic surface hopping [17] due to the nonadiabatic coupling between excitonic potential energy surfaces [18]. This approach captures exciton dynamics for the whole parameter range from the limit corresponding to completely delocalized excitons up to the other extreme where the polaron is immobilized and trapped on only one site [19].

2. Theory

According to the Born–Oppenheimer approximation we separate the electronic system from the nuclear motions. The nuclear system will be separated into explicit and bath modes. The former are assumed to be coupled to the electronic system immediately by the adiabatic potential energy surface. The bath modes will be described as statistically fluctuating external forces driving the explicit modes and damping them. Following Caldeira–Leggett, the bath modes are harmonic oscillators and the coupling between bath and explicit modes is bilinear in the coordinates q_i (see [20] for details) leading to the Langevin equation of motion in the Markov limit [21,22] for the explicit modes. For sake of simplicity, we will restrict

our considerations to aggregates of two-level molecules leading to the excitonic Hamiltonian where $\omega^{(\text{eg})}$ is the Frank–Condon transition energies and $J_{ij} = J\delta_{i,j\pm 1}$ describe the resonance interaction between the transition dipole moments of neighboring molecules. The final set of equations can be written as

$$\hat{H}_{ij} = (\omega^{(\text{eg})} - \omega dq_i)\delta_{ij} + J_{ij}(1 - \delta_{ij}), \quad (1)$$

$$\dot{p}_i(t) + \gamma p_i(t) - F_i(\dots q_i \dots) = f_i(t). \quad (2)$$

We use one explicit mode per site with the same vibrational frequency (ω) (excited as well as ground state), the displacement of the excited state potential surface is denoted d and the p_i is the nuclear momenta on site i . The Markovian friction γ and the Gaussian random force $f_i(t)$ are related by the fluctuation–dissipation relation which in the long-time limit leads to thermalized coordinate distribution, where the zero-point motions are included [23]. The exciton states are defined by the eigenvalues (E_α) and the eigenvectors ($|\alpha\rangle$) of the Hamiltonian $\langle \alpha | H | \beta \rangle = E_\alpha \delta_{\alpha\beta}$. The transformation from the real-space (molecular site) representation to the exciton-space representation can be achieved using the eigenvectors $|\alpha\rangle$ with components for i th molecule α_i . The intrinsic forces $F_i(\dots q_i \dots)$ are given by

$$F_i(\dots q_i \dots) = - \left\langle \frac{\partial U_\alpha(\dots q_i \dots)}{\partial q_i} \right\rangle, \quad (3)$$

where the potential energy surfaces are

$$U_\alpha(\dots q_i \dots) = E_\alpha + \omega \sum_k q_k^2 / 2 - \sum_k \omega dq_k \alpha_k^2 \quad (4)$$

resulting in the intrinsic forces $F_i(\dots q_i \dots) = -\omega(q_i - \sum_\alpha d\alpha_i^2)$. This force corresponds to an effective harmonic potential which is an average of the ground state and the excited state potential energy surfaces with the weight factor α_i^2 giving the contribution of the excited state. Therefore, the force F_i will depend not only on q_i but on all the other coordinates as well. This leads to the feedback which will cause a correlation between vibrational modes on different molecular sites that have a significant amplitude of the currently occupied polaron state. This self-organized correlation can induce an increase of the delocalization of

the polaron states. This issue will be addressed in a separate publication. In order to describe the nonadiabatic coupling between the eigenstates $|\alpha\rangle$ due to the explicit modes, we use the surface-hopping method [17]. In general, any time-dependent one-exciton wavefunction can be expanded in the adiabatic basis set $|\alpha\rangle$ and propagated for a short time as

$$|\Psi_{\text{tot}}(t + \Delta t)\rangle = \sum_{\alpha} C_{\alpha}(t) \exp \left[-\frac{i}{\hbar} \int_t^{t+\Delta t} U_{\alpha}(\tau) d\tau \right] |\alpha\rangle, \quad (5)$$

where $C_{\alpha}(t)$ are time-dependent expansion coefficients and Δt is the time propagation step. One has to note that the eigenstates $|\alpha\rangle$ as well as the eigenenergies $U_{\alpha}(t)$ are time-dependent due to the time dependency of the $q_i(t)$. The nonadiabatic coupling matrix is then

$$k_{\alpha\beta}(t) = \frac{i}{\hbar} \left\langle \alpha \left| \frac{\partial}{\partial t} \right| \beta \right\rangle \exp \left[i \int_0^t \omega_{\alpha\beta}(\tau) d\tau \right] \quad (6)$$

with $\omega_{\alpha\beta}(\tau) = (U_{\alpha}(\tau) - U_{\beta}(\tau))/\hbar$. In the surface hopping method, two sets of states are simultaneously followed, the reference and auxiliary states [18]. The latter are propagated coherently using the Schrödinger equation. The surface hopping probabilities are calculated from the changes of the auxiliary state populations. The reference states are propagated via the surface hopping method. The probability for hopping from state $|\alpha\rangle$ to $|\beta\rangle$ can be determined as

$$P(\alpha \rightarrow \beta) = \int_{t_0}^t (k_{\beta\alpha}(t) \rho_{\beta\alpha}(t) - k_{\alpha\beta}(t) \rho_{\alpha\beta}(t)) dt \quad (7)$$

using the notation: $\rho_{\alpha\beta}(t) = C_{\alpha}^{\dagger}(t) C_{\beta}(t)$ and where t_0 is the time of the latest hop. At each time-instant only one reference state is populated.

The surface-hopping algorithm is implemented via the following steps:

(i) The system is initialized, as the electronic Hamiltonian at time zero is generated using a randomly distributed set of coordinates and momenta, $\{q_0, p_0\}$, corresponding to the given system temperature. Note that at time zero the reference states and the auxiliary states are the same, which is not generally true for the following time steps.

(ii) The explicit mode oscillators are propagated a time step using the Langevin equation (2), the new electronic Hamiltonian is generated. The populations on the auxiliary states are propagated according to Eqs. (5) and (6).

(iii) Based on the auxiliary states the hopping probability for the reference configuration is calculated using Eq. (7). The uphill probabilities are weighted by the corresponding Boltzmann factors. The surface hopping method is executed in a Monte Carlo fashion using uniformly distributed random numbers. Continues with step (ii).

After a certain number of steps the relevant characteristics of the systems dynamics are recorded and the whole procedure is repeated. Different runs naturally leads to different trajectories. The observables are averaged over a sufficiently large set of trajectories. Bittner and Rossky [24] have studied the fundamental implications this approach in mixed quantum-classical calculations in the context of decoherence based upon the consistent histories interpretation of quantum mechanics.

3. Results and discussion

In Fig. 1, the exciton energies are displayed as a function of time for a linear aggregate consisting of $N = 6$ two-level molecules, specific model parameters are given in the figure caption. The dynamics of the exciton energies are displayed for the case where the population initially ($t = 0$) was placed on the highest exciton state. The exciton relaxation causes the population to descend to the lowest state within 100 fs. After that polaron formation can be seen, i.e. the broadening of the exciton band gap when the energy of the occupied site is decreased. The thick solid line overlaid on the exciton energies is the representation of the current populated state. In Fig. 2, the averaged exciton level dynamics is displayed for the same system as in Fig. 1, together with the averaged state occupation number (the solid black line). Two different processes readily can be identified, the exciton relaxation and the polaron formation. The exciton relaxation occurs for $t \leq 200$ fs and

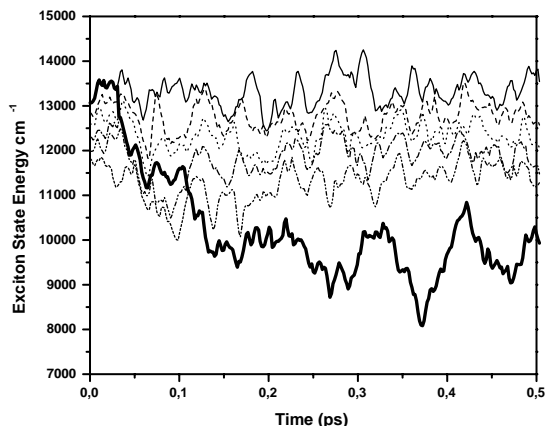


Fig. 1. The excitonic (adiabatic) level dynamics for a system with $N = 6$ identical molecules with the populated reference state overlaid (the thick solid line). The transition energies ($\omega^{(eg)}$) were set to 12400 cm^{-1} and the nearest neighbor interaction $J = 342 \text{ cm}^{-1}$. The other parameters were $\omega = 2J$, $\omega/\gamma = 1.4$, the Huang–Rhys factor $S = (1/2)d^2$ was set to 2 and $T \sim 0 \text{ K}$.

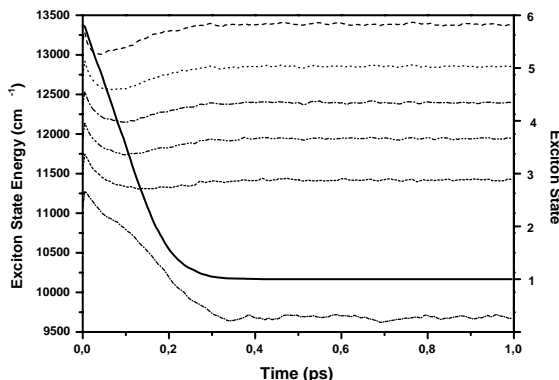


Fig. 2. The averaged exciton energies calculated for the same parameters as in Fig. 1. The solid black line displays the exciton relaxation as the averaged populated state number (right axis).

from that up to about 300 fs the polaron is formed. With the parameters the polaron is formed very rapidly. If the mode that is responsible for the polaron formation has lower frequency, one would expect slower process here. For example, in B850 polaron formation occurs in significantly slower timescale compared to the exciton relaxation [10].

In order to characterize the polaron formation and dynamics, we use the participation ratio as a measure for the polaron localization, $L_{\text{ipr}}^{-1} = \sum_{i,\alpha} \alpha_i^4 P_\alpha$, where P_α is the normalized state population. Since the polaron deforms the surrounding lattice, its mobility, compared to an exciton, is lower. This decrease of mobility occurs due to the strong exciton–phonon coupling. Following Mak and Egger [25], the polaron position operator can be defined as $Q(t) = \sum_i \rho_{ii}(t) * i$. Using the position operator we introduce the polaron velocity as $I(t) = |\partial Q(t)/\partial t|$. The inverse participation ratio together with the polaron velocity capture the characteristics of the polaron formation and dynamics. The exciton can be localized on a part of the aggregate without the formation of a polaron, but if the exciton is both localized and the velocity is significantly reduced we conclude that polaron

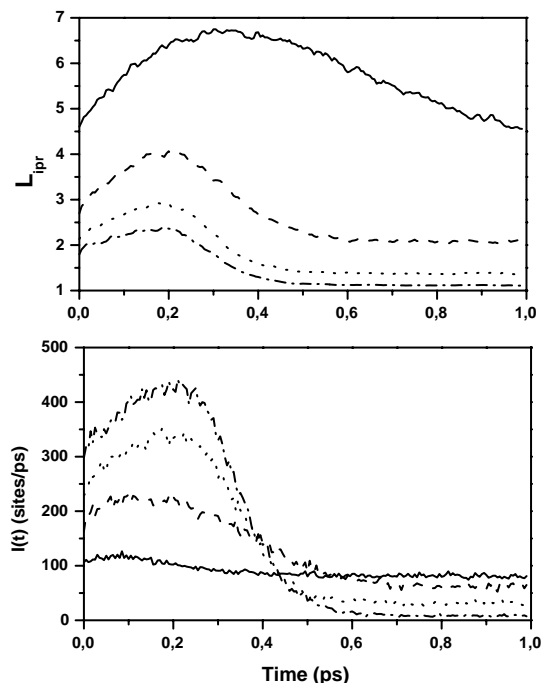


Fig. 3. The inverse participation ratio (top) and the polaron velocity (bottom) is displayed for four different displacement coordinates as a function of time. The curves correspond to the Huang–Rhys factors (solid, $S = 0.125$), (dash, $S = 0.5$), (dot, $S = 1.125$) and (dash-dot, $S = 2$). The rest of the parameters are the same as in Fig. 1.

formation has occurred. In Fig. 3 the inverse participation ratio (L_{ipr}) in the top panel and the polaron velocity ($I(t)$) in the bottom panel are displayed for four different Huang–Rhys factors. Here the system size is increased to 14 two-level molecules. The initial values reflect the initial thermal distribution of the explicit modes, corresponding to an effective static disorder. It is important to notice the initial rise of the inverse participation ratio ($L_{\text{ipr}}(t)$). This increase during the exciton relaxation process is an effect of the different inverse participation ratios of the exciton states [26] due to the disorder. Besides, the vibrational coupling may change the localization of the exciton wavefunction [27]. Both effects are most prominent in the exciton band edges. So that during the relaxation process the averaged total inverse participation ratio is highest when the states in the center of the exciton band are populated. The exciton relaxation, as seen in Figs. 1 and 2, can be seen in Fig. 3 as the initial rise of both the inverse participation ratio (L_{ipr}) and the polaron velocity ($I(t)$). The trace in Fig. 3 with the same parameters as for Figs. 1 and 2 reproduces the same timescale even for these measures. Further, it can be seen from Fig. 3 that the processes are slower for a decreased exciton–vibrational coupling (smaller S). After the exciton relaxation, both the inverse participation ratio and the polaron velocity decay towards their respective equilibrium values, depending on the ratio between the Stokes shift ($2S\omega$, where ω is the mode frequency) and the intermolecular resonance interaction (J). Beenken et al. [27] have thoroughly studied the localization properties and polaron formation for an extensive set of the above ratio in excitonic dimers.

The increase of the initial velocity $I(t)$ with increasing exciton–phonon coupling is an effect of the decrease of delocalization length of the polaron. The stronger coupling leads to the smaller polaron and during the initial period the center of gravity of the polaron has to move over the aggregate in order to relax from state to state.

The polaron formation is shown as polaron state energy evolution in Figs. 1 and 2 and as a change of the polaron velocity in Fig. 3. In order to study the details of polaron migration, we pre-

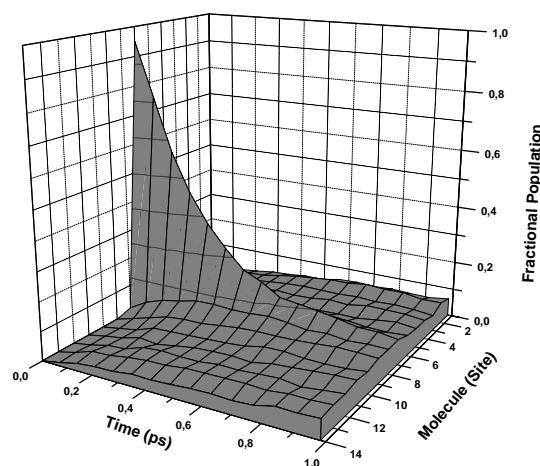


Fig. 4. Time-dependence of the excitation probability in site representation. The polaron is initially placed on site 7. Due to a random walk type migration the initial population decays with a time constant of 0.5 ps. $S = 2$, all other parameters as in Fig. 3.

pared an initial state corresponding to a self-trapped polaron on a specific site of the molecular aggregate. Fig. 4 displays the polaron migration away from the initially populated site eventually leading to an uniform distribution over the entire aggregate. This shows that the polaron motion within the molecular aggregate has a random walk character where the properties depend on the intermolecular interaction in conjunction with the vibrational frequencies and the exciton–vibrational coupling.

In summary, we have presented a novel method for calculating exciton dynamics in molecular aggregates. Such phenomena as polaron formation and self-trapping can readily be accounted for.

Acknowledgements

This work was financially supported by the Swedish Research Council and the Wenner-Gren foundation.

References

- [1] H. van Amerongen, L. Valkunas, R. van Grondelle, *Photosynthetic Excitons*, World Scientific, Singapore, 2000.

- [2] S. Higai, H. Sumi, *J. Phys. Soc. Jpn.* 63 (1994) 4489.
- [3] Y. Toyozawa, in: C.G. Kuper, G.D. Whitfield (Eds.), *Polarons and Excitons*, Oliver & Boyd, Edinburgh, 1963, p. 211.
- [4] H. Fröhlich, in: C.G. Kuper, G.D. Whitfield (Eds.), *Polarons and Excitons*, Oliver & Boyd, Edinburgh, 1963, p. 1.
- [5] D. Emin, T. Holstein, *Phys. Rev. Lett.* 36 (1976) 323.
- [6] E.I. Rashba, *Opt. Spektrosk.* 2 (1957) 88.
- [7] D.W. Brown, K. Lindenberg, B.J. West, *J. Chem. Phys.* 84 (1986) 1574.
- [8] V. Sundström, T. Pullerits, R. van Grondelle, *J. Phys. Chem. B* 103 (1999) 2327.
- [9] M. Dahlbom, T. Pullerits, S. Mukamel, V. Sundström, *J. Phys. Chem. B* 105 (2001) 5515.
- [10] T. Polivka, T. Pullerits, J.L. Herek, V. Sundström, *J. Phys. Chem. B* 104 (2000) 1088.
- [11] K. Timpmann, Z. Katiliene, N.W. Woodbury, A. Freiberg, *J. Phys. Chem. B* 105 (2001) 12223.
- [12] M. Dahlbom, T. Minami, V. Chernyak, T. Pullerits, V. Sundström, S. Mukamel, *J. Phys. Chem. B* 104 (2000) 3976.
- [13] O. Kühn, V. Sundström, *J. Phys. Chem. B* 101 (1997) 3432.
- [14] O. Kühn, V. Sundström, T. Pullerits, *Chem. Phys.* 275 (2002) 15.
- [15] A. Damjanovic, I. Kosztin, U. Kleinekathöfer, K. Schulten, *Phys. Rev. E* 65 (2000) 031919.
- [16] T. Meier, Y. Zhao, V. Chernyak, S. Mukamel, *J. Chem. Phys.* 107 (1997) 3876.
- [17] J.C. Tully, *J. Chem. Phys.* 93 (1990) 1061.
- [18] K.F. Wong, P.J. Rossky, *J. Phys. Chem. A* 105 (2001) 2546.
- [19] M. Dahlbom, W. Beenken, V. Sundström, T. Pullerits, *The Proceedings of BioPhysical Chemistry 2001*, London, 2002 (in press).
- [20] I.B. Bersuker, V.Z. Polinger, *Vibronic Interaction in Molecules and Crystals*, Springer, Berlin, 1998.
- [21] U. Weiss, *Quantum Dissipative Systems*, World Scientific, Singapore, 1999.
- [22] A.O. Caldeira, A.J. Leggett, *Ann. Phys. (NY)* 149 (1983) 374.
- [23] S. Mukamel, *Principles of Nonlinear Optical Spectroscopy*, Oxford University Press, New York, 1995.
- [24] E.R. Bittner, P.J. Rossky, *J. Chem. Phys.* 107 (1997) 8611.
- [25] C.H. Mak, R. Egger, *Phys. Rev. E* 49 (1994) 1997.
- [26] H. Fidder, J. Knoester, D. Wiersma, *J. Chem. Phys.* 95 (1991) 7880.
- [27] W. Beenken, M. Dahlbom, P. Kjellberg, T. Pullerits, *J. Chem. Phys.* 117 (2002) 5810.